Continuous observations of Asian dust and other aerosols by polarization lidars in China and Japan during ACE-Asia

Atsushi Shimizu,[1] Nobuo Sugimoto,[1] Ichiro Matsui,[1] Kimio Arao,[2] Itsushi Uno,[3] Toshiyuki Murayama,[4] Naoki Kagawa,[5] Kazuma Aoki,[6] Akihiro Uchiyama,[7] and Akihiro Yamazaki[7]

Received 30 November 2002; revised 8 September 2003; accepted 6 October 2003; published 6 August 2004.

[1] Continuous observations of aerosols in China and Japan were made by polarization lidars during March to May 2001, corresponding with the Asian Pacific Regional Aerosol Characterization Experiment (ACE-Asia) field campaign period. Lidars in Beijing, Nagasaki, and Tsukuba were continuously operated regardless of weather conditions. Scatterers in the atmosphere were categorized for all vertical profiles, and occurrence frequencies of dust, spherical aerosols, and clouds up to 6 km were calculated. The frequency of dust was highest in Beijing for the whole height range. There was a peak of dust occurrence near the ground in Nagasaki. Dust was frequently detected in the free troposphere in Tsukuba. The contributions of dust and spherical aerosols to the total backscattering coefficient were estimated from the depolarization ratio with the assumption of the external mixture of both kinds of aerosols. Vertical profiles of backscattering by dust and by spherical aerosols represented the different characteristics of these aerosols. The monthly averaged backscattering coefficients by dust near the surface were 0.003/km/sr in Beijing, 0.001–0.002/km/sr in Nagasaki, and 0.0006/km/sr in Tsukuba. The backscattering coefficients by spherical aerosols near the surface were 0.002–0.004/km/sr at all three observatories. We compared the derived backscattering coefficients with aerosol mass concentrations calculated by a numerical model, Chemical Weather Forecasting System (CFORS). CFORS reproduced well the vertical structures of the tall dust events and the enhancements of spherical aerosols throughout the observation period. A specific dust event on 16–19 May 2001 was analyzed by using five lidars in Japan, and its fine structure is described. *INDEX TERMS:* 0305 Atmospheric Composition and Structure: Aerosols and particles (0345, 4801); 0368 Atmospheric Composition and Structure: Troposphere—constituent transport and chemistry; 3309 Meteorology and Atmospheric Dynamics: Climatology (1620); 3360 Meteorology and Atmospheric Dynamics: Remote sensing; *KEYWORDS:* continuous lidar observation, dust transport, depolarization ratio

Citation: Shimizu, A., N. Sugimoto, I. Matsui, K. Arao, I. Uno, T. Murayama, N. Kagawa, K. Aoki, A. Uchiyama, and A. Yamazaki (2004), Continuous observations of Asian dust and other aerosols by polarization lidars in China and Japan during ACE-Asia, *J. Geophys. Res.*, *109*, D19S17, doi:10.1029/2002JD003253.

1. Introduction

[2] Asian dust (yellow sand, kosa) is a dominant aerosol component in spring in east Asia. It is generated in the interior of Eurasia (Inner and Outer Mongolia and the Takla Makan desert) and blown eastward, over the Pacific [*Sugimoto et al.*, 2002], sometimes reaching North America [*Husar et al.*, 2001; *Uno et al.*, 2001]. The dust affects not only the local air quality, but also the local radiative forcing [*Myhre and Stordal*, 2001]. Anthropogenic aerosols play a similarly important role. In these years, several coordinated scientific programs were carried out to accurately assess the radiative effects by these aerosols in several regions in the world. The Indian Ocean Experiment (INDOEX) focused on the aerosols over south Asia and North Indian Ocean [*Ramanathan et al.*, 2001]. In this campaign, vertical profiles of optical properties were obtained by six-wavelength lidar [*Müller et al.*, 2001] where backscatter and extinction coefficients, and lidar ratios were precisely reported. *Pelon et al.* [2002] also described vertical profiles of extinction

[1]National Institute for Environmental Studies, Ibaraki, Japan.
[2]Faculty of Environmental Studies, Nagasaki University, Nagasaki, Japan.
[3]Research Institute for Applied Mechanics, Kyushu University, Fukuoka, Japan.
[4]Department of Physics, Tokyo University of Mercantile Marine, Tokyo, Japan.
[5]Faculty of Engineering, Fukuyama University, Hiroshima, Japan.
[6]Faculty of Education, Toyama University, Toyama, Japan.
[7]Meteorological Research Institute, Ibaraki, Japan.

0148-0227/04/2002JD003253

coefficient during INDOEX retrieved by airborne lidar, and estimated the single scattering albedo of aerosols. As for the aerosols over North Atlantic Ocean, Tropospheric Aerosol Radiative Forcing Observational Experiment (TARFOX) was conducted [*Russell et al.*, 1999], where the importance of carbonaceous compounds was demonstrated.

[3] The Asian Pacific Regional Aerosol Characterization Experiment (ACE-Asia) is being conducted to determine the effect of these aerosols on the climate in east Asia. Intensive ground, shipboard, airborne, and satellite observations were carried out in spring 2001, and some numerical models were used to predict or analyze the three-dimensional distribution of aerosols in this region. Almost in the same region, Atmospheric Particulate Environment Change Studies (APEX) has been conducted since 2001 and still be continued.

[4] Lidar measurements of Asian dust have been taken for more than 20 years and used to describe the vertical distribution of the aerosol layer [*Iwasaka et al.*, 1983, 1988]. One purpose of such studies is to identify the region of dust origin. The height and time of a dust plume's arrival at the lidar observatory are determined, and the backward trajectory is calculated to infer the origin. Polarization lidar, which can determine the depolarization ratio of the backscattering signal, is a powerful instrument for studying the optical properties of dust aerosols. *Murayama et al.* [1999] demonstrated the usefulness of polarization lidar observations combined with ground measurements to investigate the characteristics of aerosol particles in the boundary layer. *Sakai et al.* [2000] presented results of long-term lidar observations of the depolarization ratio and relative humidity and discussed the contributions of various species of aerosols to the air mass over Nagoya, Japan.

[5] Recently, lidar systems were installed widely throughout east Asia [*Murayama et al.*, 2001] and were operated intensively during the ACE-Asia Intensive Observation Period (IOP). Commonly, the lidar observations are started and stopped by an operator on fine days. However, for comparison with numerical models, nonstop operation of the lidar is desirable because the atmospheric phenomena occurs continuously in the model and an intermittent observation may miss some important events. Also, as numerical models calculate the concentration of each aerosol component, observations are needed to estimate the contribution of each aerosol species to the total backscattering coefficient. In this paper we describe the utility of polarization lidar measurements for distinguishing mineral dust and spherical aerosols, and compare these measurements with dust and sulfate concentrations calculated by a numerical model.

[6] We conducted continuous lidar observations in Japan and China during the ACE-Asia IOP. The lidar system is described in section 2. Statistical analysis of the lidar data obtained in Tsukuba, Nagasaki, and Beijing is described in section 3. Comparison with a numerical model and description of the fine structure of a dust event in Japan in May 2001 are discussed subsequently and finally concluding remarks are presented.

2. Observation Method

[7] The National Institute for Environmental Studies (NIES) began continuous observation of the atmosphere in 1996 in Tsukuba, Japan, with a compact Mie-scattering lidar system, and added polarization measurement capability in 1999. Similar systems were installed at Nagasaki University on 22 February 2001 and at the Sino-Japan Friendship Center for Environmental Protection in Beijing on 1 March 2001. The alignment of the laser beam and the telescope at Nagasaki was poor, so data collected before 12 March were excluded from this study.

[8] All the lidars utilize the second harmonics (532 nm) of a flashlamp-pumped Nd:YAG laser as a light source. The energy of laser is 50 mJ, and the light is emitted vertically with a pulse repetition of 10 Hz. Telescopes with a diameter of 35 cm (Tsukuba), 30 cm (Nagasaki) or 20 cm (Beijing) are used to collect the scattered light from the sky at an observation wavelength of 532 nm. Each system has two photomultiplier tubes to detect both parallel and perpendicular polarized components which are separated by a cubic polarizer. In this paper we define the total (observed) depolarization ratio, δ as

$$\delta = P_{\perp}/P_{\parallel}$$

where $P_{\perp}$ and $P_{\parallel}$ are the backscattering signal intensity of perpendicular and parallel components, respectively. In order to cancel the different sensitivity of two photomultiplier tubes, a seat polarizer whose polarizing direction is inclined 45° to that of the cubic polarizer is inserted before the collected light enters the cubic polarizer to obtain profiles for the calibration. In these profiles, $P_{\perp}$ and $P_{\parallel}$ become equivalent regardless of scatterer in the sky, and we can compare sensitivities of two photomultiplier tubes. A digital oscilloscope is used to digitize the output from the photomultiplier tubes, at a sampling rate of 25 MHz. The range resolution of the lidar system is 6 m, and data were recorded up to 24 km (4000 points). Although the resolution of the digital oscilloscope is 8 bits, if we repeat measurements of profiles with dithering noise, averaged profile shows an improved resolution [*Shimizu et al.*, 1981]. Because the output from photomultiplier tubes are contaminated with such noise, by averaging 100 independent profiles during 10 s we obtain 11–12 bit resolution for the averaged (10 s) profile. The overlap of the laser and the field of view of the telescope is compensated below 600 m using a vertical compensation function, which was determined by observed profiles during conditions when well-mixed boundary layer is expected.

[9] A Linux-based PC controls each system, starting the laser, recording the output from the oscilloscope to hard disk, and stopping the laser. One profile, comprising 3000 shots, is obtained in 5 min, followed by a 10-min rest. This intermittent operation is intended to maintain the laser life without the need for frequent maintenance. Signal-to-noise ratios (SNR) at 6 km height after accumulating 3000 shots in the clear sky condition were about 40, 20, 10 at Tsukuba, Nagasaki and Beijing, respectively. Differences of diameter of telescope and lower atmospheric conditions caused this difference in SNR. The lidar system is installed in a container or a room with a transparent glass roof. This ensures its operation in all weather conditions. Low-quality data caused by bad weather are rejected in the data analysis process. Owing to the automated control, the system can be operated without the attendance of staff, although the glass roof needs to be wiped by hand every few days.

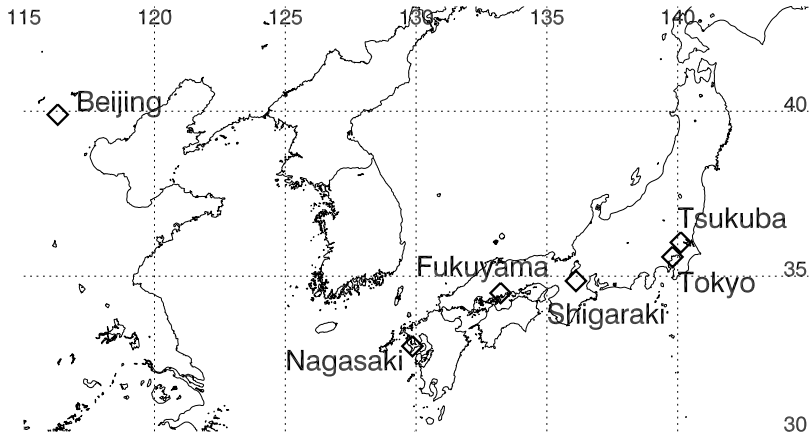

Figure 1. Locations of lidar observatories in China and Japan.

[10] Data from Nagasaki and Tsukuba are transferred to NIES just after each observation via the Internet, and quick-look figures of backscattering intensity and depolarization ratio are shown on the NIES lidar team's Web page. The PCs can also be controlled from NIES via the Internet. The Beijing lidar is not connected to the Internet, and data are transferred on CD-ROM. Vertical profiles of backscattering intensity and depolarization ratio were recorded every 15 min from March to May 2001.

[11] The lidar data presented in section 4.2 were provided by the Tokyo University of Mercantile Marine, Fukuyama University, and Kyoto University. These lidar systems have a polarization capability and the observation wavelength is 532 nm. The time/height resolution is dependent on the observatories. All of the location of these lidar systems are presented in Figure 1.

3. Statistics of Vertical Distribution of Aerosols

[12] The continuous lidar results in Beijing, Nagasaki, and Tsukuba were analyzed in two ways. The scatterers were categorized by the vertical shape of the lidar signals for all profiles. This is a powerful method that does not depend on any assumptions to solve the lidar equation. In contrast, quantitative analysis was used for profiles collected on clear days. Although the total number of profiles analyzed is reduced with this method, the results are useful for giving averaged backscattering profiles, and for comparing with numerical model results.

3.1. Categorization of Scatterers for All Days

[13] The scatterers in the atmosphere are inferred from the vertical structures of both range-corrected intensity and depolarization ratio. Although this analysis is qualitative, it can treat as many profiles as desired, because it makes no assumptions about boundary conditions.

[14] All the time-height data are classified into seven categories: (1) nonobservation, (2) unknown, (3) spherical aerosols, (4) mineral dust, (5) water cloud, (6) ice cloud, and (7) rain or snow. As for naming of "mineral dust," strict expression may be "nonspherical aerosols" because it is identified only from the shape of particles. Since mineral dust is considered as the most important component of nonspherical aerosols in east Asia, hereafter we labeled it as mineral dust.

[15] First, the steep vertical gradient of the range-corrected intensity is used to detect the cloud base in the profile. If the signal intensity increases more than 7.2%/m within 6 m vertical layer and this condition is satisfied in three successive points, this height is judged as a cloud base. If a very thin and obscure cloud exists, this method cannot detect the cloud base. Also, it should be noted that very steep edge of an aerosol layer might be judged as a cloud base. If the cloud base is detected, the apparent cloud top is determined by finding the height where the signal intensity becomes again equal to that of cloud base. The cloud is classified as water cloud or ice cloud on the bases of the depolarization ratio between the cloud base and the cloud top. The threshold value is 20%. As the lidar signal is weak above the cloud top, we do not classify that region and we treat the scatterers there as unknown. If the range-corrected signal below 900 m contains a lot of negative data, the whole profile is treated as rainy or snowing. This nature comes from the characteristics of our photomultiplier tubes. They show negative output just after very strong scattering light from the water layer on the glass roof. Although this is empirical method and not straightly utilized for all of lidar observations, the classification by lidar agrees well with ground observation of rainfall in our cases. Scatterers in clear sky or below the cloud base are divided into two categories. If the depolarization ratio of the region is less than 10% it is identified as spherical aerosol, and if it exceeds 10% it is identified as mineral dust. The threshold values of 10% for the aerosols and 20% for the clouds are arbitrary and determined empirically. Although 10% is large for a single spherical particle, in this case the term of spherical aerosol means an air mass which contains spherical particles dominantly. We employed 20% to separate water and ice clouds since a histogram of the all depolarization data in clouds has two peaks around a few percent and 30%. However, there may be still ambiguity of phase of cloud using a fixed threshold value.

[16] The time-height sections of scatterers below 6 km at Beijing, Nagasaki, and Tsukuba in April 2001 are displayed in Figure 2. Characteristics of the vertical and temporal distributions of the clouds and aerosols are clearly seen. In Beijing, mineral dust was frequently detected near the surface, and sometimes the top of the dust layer reached 3–4 km. Each dust event continued for several days. Surface dusts were identified in Nagasaki, too. They

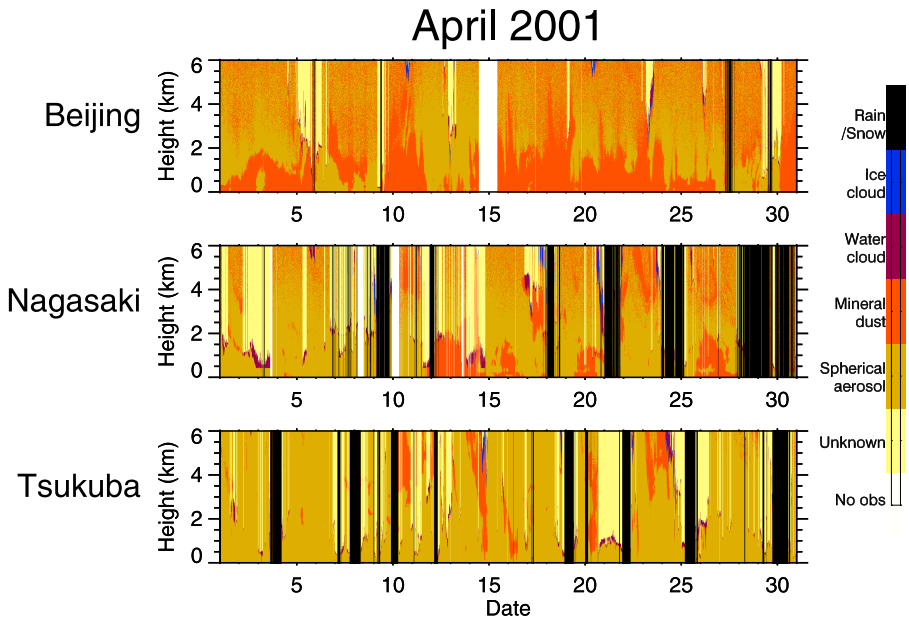

Figure 2. Time-height sections of scatterers below 6 km in April 2001.

occurred a few days after the dust occurrences in Beijing. For example, dust event was detected on 13 April in Nagasaki, and there was a dust event on 10 April in Beijing in advance. Details of advection of dust layers in this period are studied by *Murayama et al.* [2002] with results from other lidars and satellite observations. The horizontal advection of dust is confirmed from results of a numerical model mentioned in section 4. Floating dusts were also

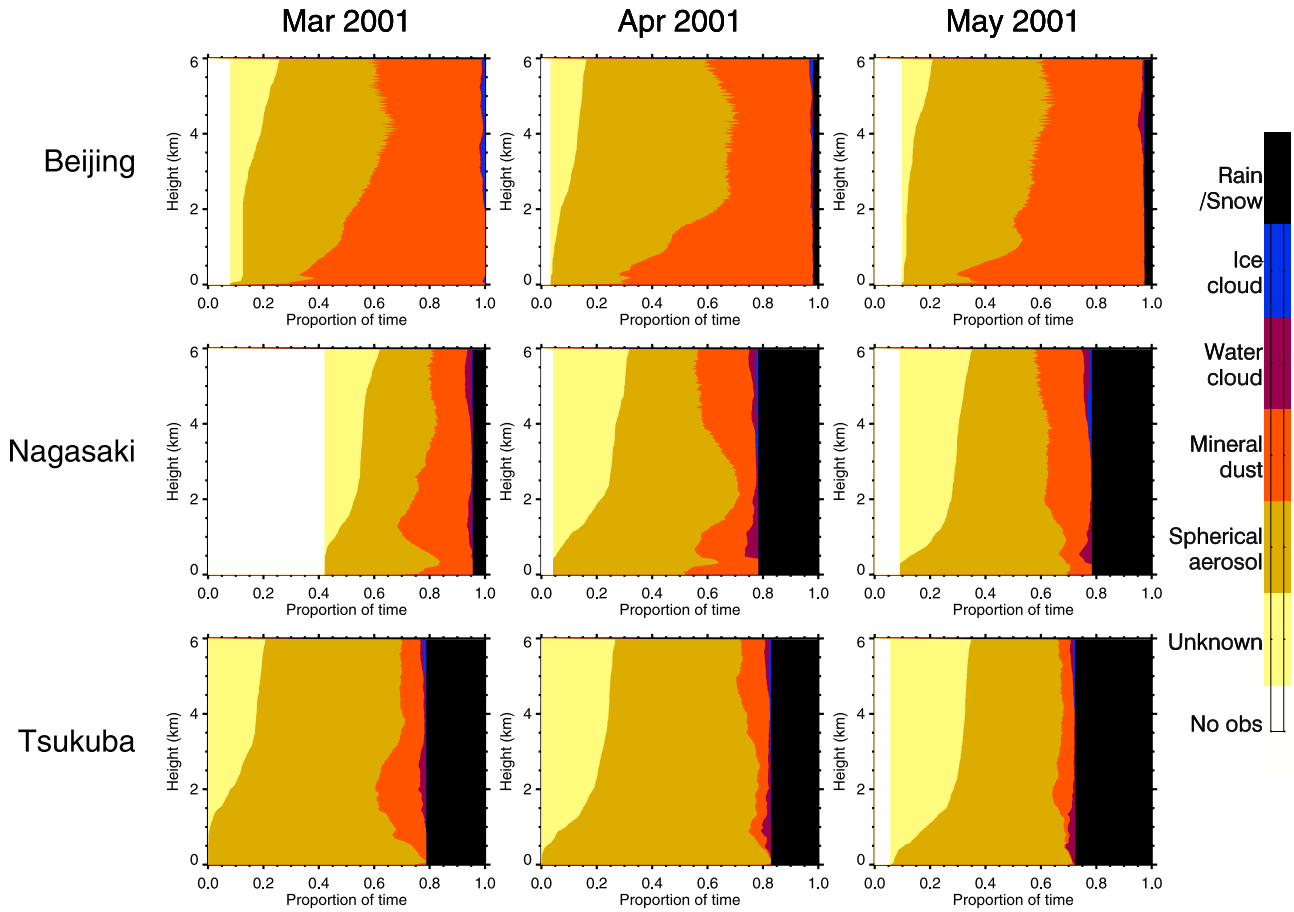

Figure 3. Proportion of each scatterer at each height in 2001, based on Figure 1. Each area is based on the ratio of total time for each scatterer to the total time of observation.

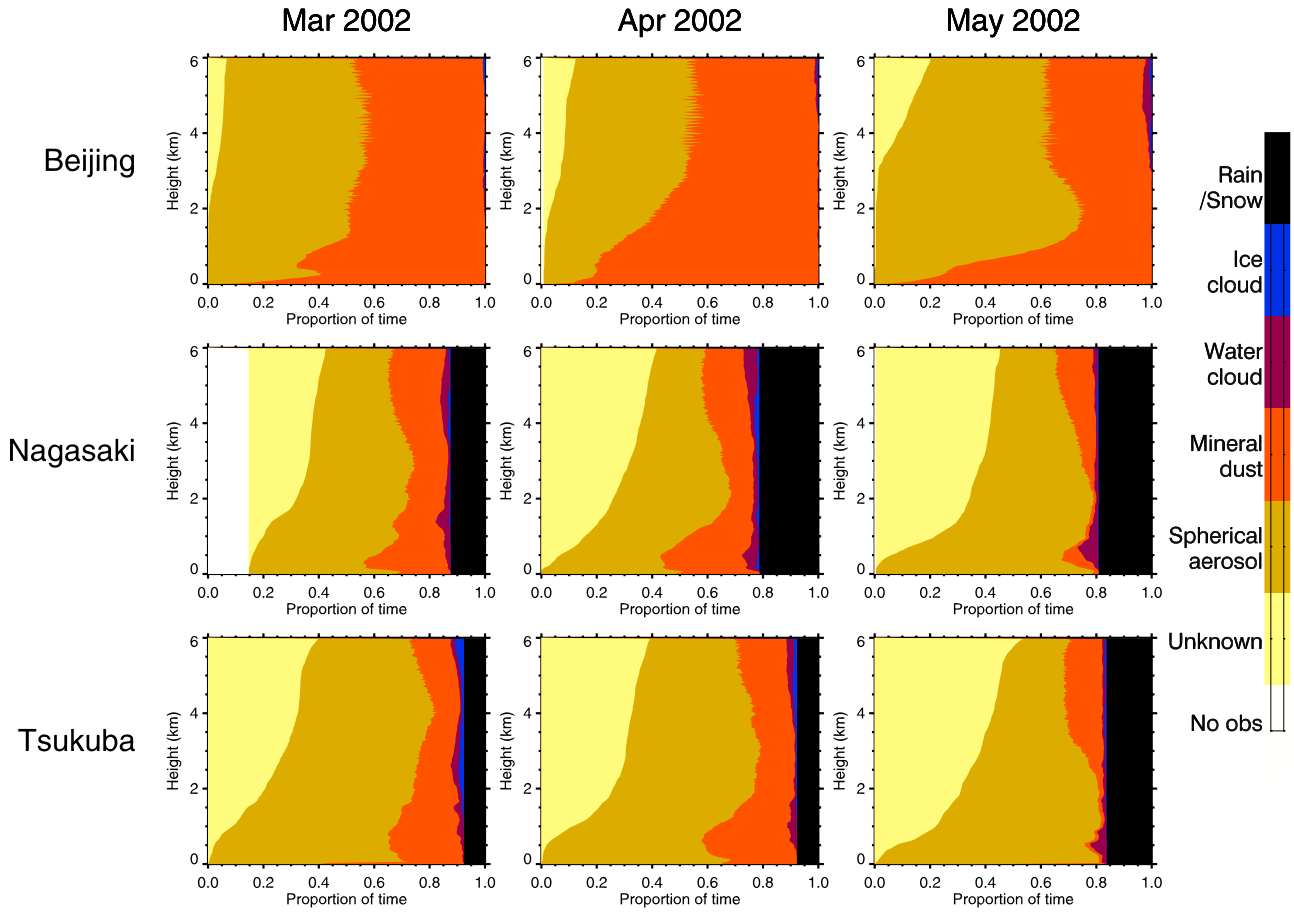

Figure 4. Same as Figure 3, but for 2002.

detected in Nagasaki, for example, on 10, 17 and 23 April. However, dust near the surface was seldom seen in Tsukuba, although floating dust in the free troposphere was detected several times. The occurrences of the floating layer corresponded between Nagasaki and Tsukuba, with a time difference of about a day on 23–24 April.

[17] The total duration of occurrences of each category at each height during 1 month was counted. Then the durations of all categories were sorted and displayed as histograms. Histograms for March, April, and May 2001 are presented in Figure 3. In Beijing the dust was detected for more than 60% of total observation time. In the free troposphere the duration of dust detection was around 40%. There was very little cloud and rain. The characteristics of occurrences of dust were very similar during March and May.

[18] Dust occurrence differed between Nagasaki and Tsukuba. In Nagasaki, a lot of dust was detected at 1 km in March and April. The duration of dust occurrence was less than in Beijing. Clouds were occasionally detected around 1 km, and the cloud base height was lower in April and May than in March. In Tsukuba, there was a slight enhancement of dust around 2 km in March. However, the duration of dust occurrence in Tsukuba was lower than at the other 2 observatories at all heights. The height distribution of the cloud was similar in Nagasaki and Tsukuba.

[19] Figure 4 shows the results for 2002. The duration of dust occurrence in Beijing near the surface was greater than in 2001. The distribution was the same in Nagasaki and Tsukuba in March and April 2002, and very low in May. The dust transport to Japan seems to have finished during April. In May 2002 Tibetan high was weak and Siberian low moved eastward. As a result the horizontal wind became weak and transport of dust was not significant. So that we understand the natural variability in dust levels it is important to describe the differences between years, and the continuous observation is indispensable to this.

3.2. Quantitative Analyses for Clear Days

[20] If a profile contained no cloud up to 6 km, quantitative analysis was also done. Fernald's method was used to obtain the vertical profile of the backscattering coefficient of aerosols (β_a) using the total signal intensity ($P_{\parallel} + P_{\perp}$) [*Fernald*, 1984]. A fixed extinction-to-backscatter ratio (S1 value, or "lidar ratio") was used in the calculation. This values largely depends on its origin and size distribution [*Mattis et al.*, 2002]. As the dominant aerosol in this analysis was Asian dust, we used 50 sr as S1 [*Liu et al.*, 2002]. Hereafter we present β_a for the optical index of aerosols because it is not seriously affected by a rough estimation of S1 [*Fernald*, 1984]. However, it should be noted that extinction coefficient estimated roughly by ($\beta_a \times S1$) is also important index to compare lidar results with other optical measurements because no other equipments can retrieve backscattering coefficient. The boundary condition of the inversion calculation was set at 6 km, and Rayleigh scattering from atmospheric molecules was

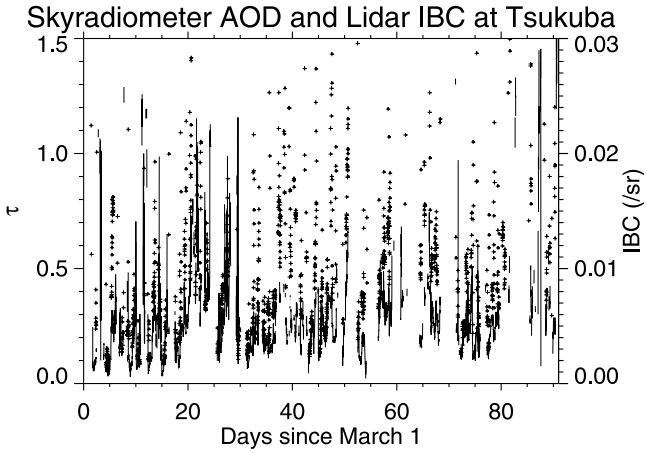

Figure 5. Optical depths (τ) obtained by sky radiometer (500 nm, crosses) and integrated backscattering coefficient (IBC) derived from lidar (532 nm, solid lines) in Tsukuba. Sky radiometer results are averaged over 15 min for comparison with lidar results.

obtained from the atmospheric density profile in the U.S. Standard Atmosphere (1976). Uncertainty of β_a is almost 5% near the ground when the SNR equaled to 10 at 6 km and β_a was 0.006/km/sr at 600 m (Beijing case). Sometimes there was an aerosol layer at 6 km, and profile of β_a showed negative value in the lower troposphere. In such cases we employed a nonzero value of β_a at the boundary height, (the value was proportional to the absolute value of negative peak of β_a) and calculated β_a again. This methods may cause underestimation of β_a if aerosols were distributed compactly between surface and 6 km. However, in almost cases aerosol layer at 6 km was floated one and an aerosol free layer existed below that. This condition leads our method to obtain reasonable β_a. From Figure 2, we can identify two floated dust layers around 6 km height on 10 and 23 April. Differences between β_a by normalization at 9 km and β_a by normalization at 6 km with our compensation method were about 6% at 5.4 km and 2% at 600 m for 10 April case. However, for 23 April case they were 25% and 15%, respectively. These results imply a limitation of our method for some cases.

[21] To verify the validity of the inversion of lidar signals, we compared the integrated backscattering coefficient (IBC) by lidar with the aerosol optical depth (AOD) obtained by sky radiometers. In Tsukuba the sky radiometer POM-01 is installed at the Meteorological Research Institute close to NIES. In Nagasaki, the sky radiometer POM-01MK1 and lidar system were installed at the same campus of Nagasaki University. No sky radiometer observations were made in Beijing.

[22] Figure 5 shows the time variation of IBC by lidar and AOD by sky radiometer in Tsukuba. The patterns resembled each other, but the sky radiometer values were sometimes very large, especially in April. The difference in variations was smaller on optically thin days. We infer that the discrepancy is caused by the height range of lidar analysis. The IBC by lidar is the backscattering coefficient vertically integrated between the surface and 6 km. If some aerosols occur above 6 km, or thin cirrus clouds occur in the upper troposphere, they will contribute only to the sky radiometer AOD. For example, elevated dust layers were confirmed from depolarization ratio around 6 km height on 20 March, 10 and 14 April (see Figure 2), and 4 May. Upper part of these dust layers would contribute to sky radiometer AOD only. Figure 6 shows the comparison for Nagasaki where the variations agreed well. The lowest AOD was 0.2 in the absence of dust. In dust events it exceeded 1. Figure 7 is a scattering diagram for lidar IBC and sky radiometer AOD. If both AOD and IBC were calculated in same height layer, ratio between them represents mean S1 value. In Tsukuba minimum ratio is about 50 sr, and it gradually becomes larger as AOD increases. This suggests that the upper limit of 6 km in lidar analysis caused under estimate of IBC, or cloud contamination in AOD was large. In Nagasaki, the ratio is scattered around S1 = 50 sr for optically thin and thick conditions. It is plausible that the aerosols were almost concentrated below 6 km and higher clouds were well rejected by sky radiometer in Nagasaki.

[23] Although the total depolarization ratio (δ) is used for the categorization, this value depends on the density of aerosols, decreasing as the aerosols decrease. For estimating the contribution by nonspherical particles to the total backscattering, the aerosol depolarization ratio (δ_a) is a more appropriate index. δ_a is estimated from the scattering ratio, which is derived from the backscattering coefficient (β_a) [*Browell et al.*, 1990]:

$$\delta_a = \frac{\delta(BR + BR \times \delta_m - \delta_m) - \delta_m}{BR - 1 + BR \times \delta_m - \delta}, \quad (1)$$

where BR is scattering ratio ($(\beta_a + \beta_m)/\beta_m$, β_m: backscattering coefficient of atmospheric molecules), and δ_m is the depolarization ratio of atmospheric molecules (0.014 here). Histograms of the δ_a of air masses whose backscattering exceeded 0.0008/km/sr are shown in Figure 8. In Beijing, the δ_a distribution centered on 0.15–0.2, with a broad range. There was no peak below 0.1, unlike in Nagasaki and Tsukuba. This broad distribution shows that the air always contained both nonspherical (dust) and spherical particles in Beijing. In Nagasaki and Tsukuba, a minor secondary peak appeared around 0.3–0.4 in May, and values below 0.02 were very scarce.

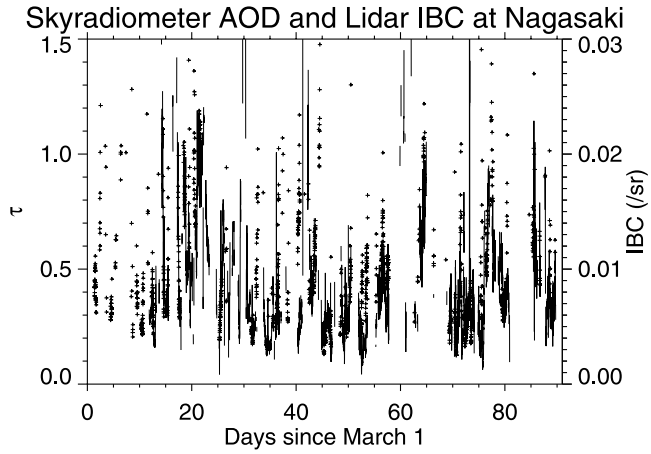

Figure 6. Same as Figure 5, but for Nagasaki.

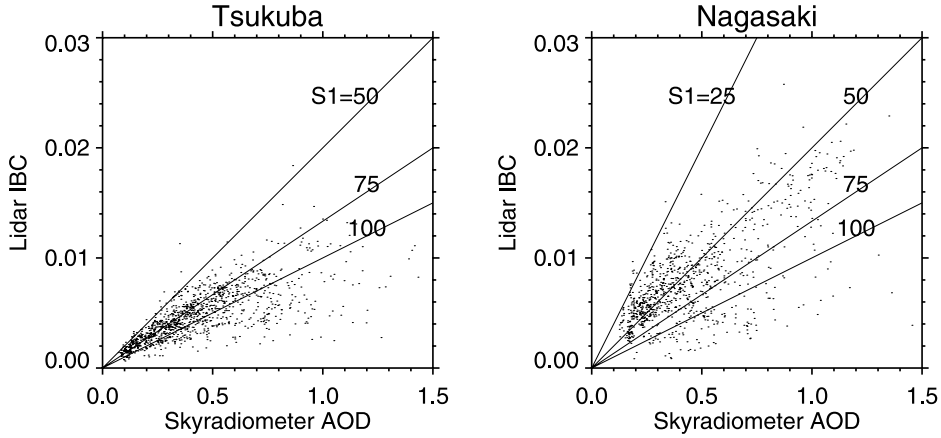

Figure 7. Scattering diagrams of τ and IBC at (left) Tsukuba and (right) Nagasaki. Solid lines indicate various ratios between them, corresponding to the lidar ratio (S1) if the aerosol concentration above 6 km can be ignored.

[24] The contribution ratio of the dust to the total backscattering is calculated from the δ_a. Although this quantity cannot be compared with results from any other instrument, it can be compared with the output of a numerical model. To separate the dust contribution, we assumed that there are only two kinds of aerosol in an air mass and they are externally mixed. At present we cannot consider intermediate particles like dust coated with water or dust contaminated by soot. In the external mixture of nonspherical particles whose δ_a is δ_1 and spherical particles whose δ_a is

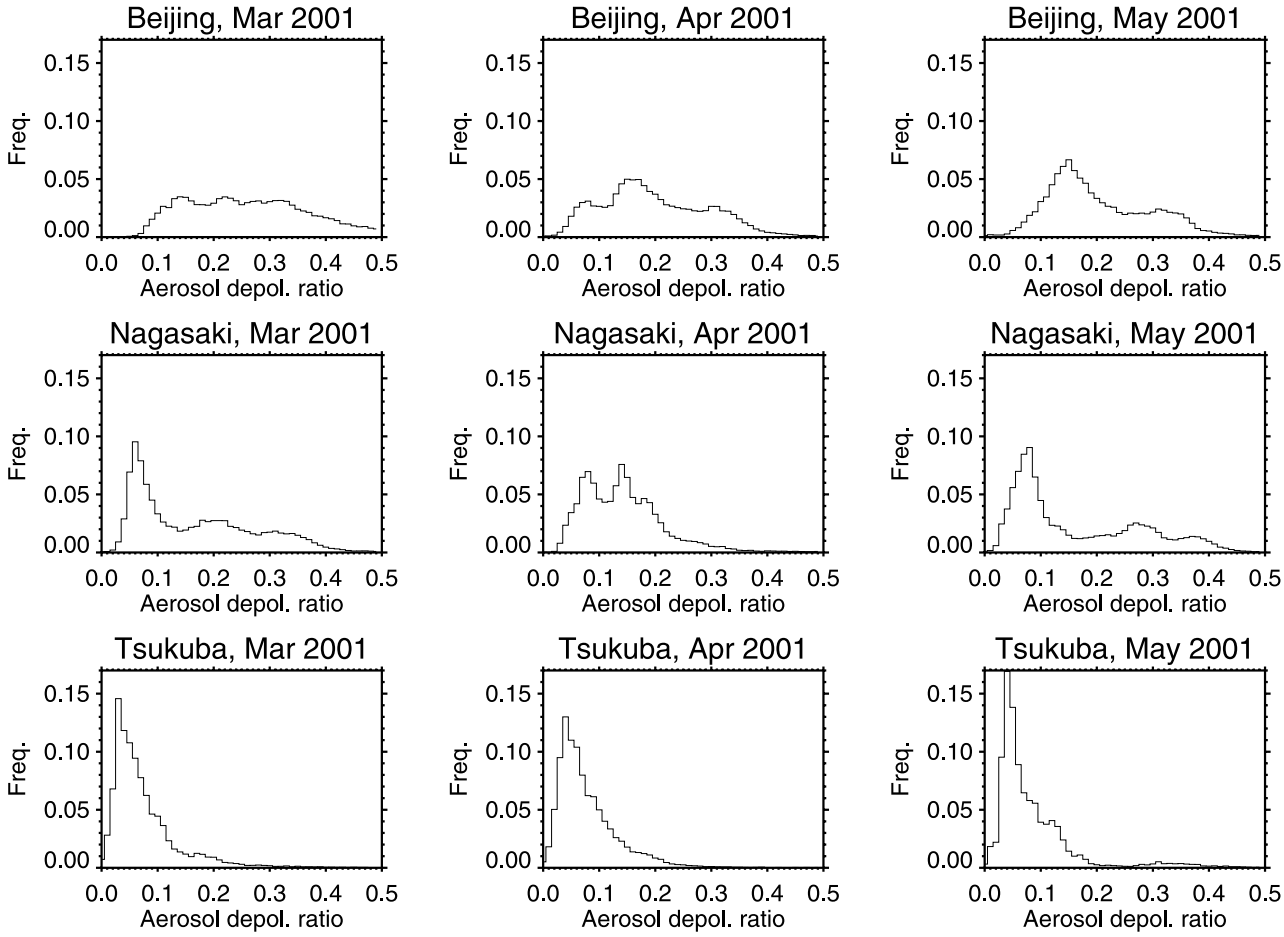

Figure 8. Histograms of the frequency of estimated aerosol depolarization ratio (δ_a) in 2001. Only data where the aerosol backscattering coefficient between the surface and 6 km exceeded 0.0008/km/sr were counted.

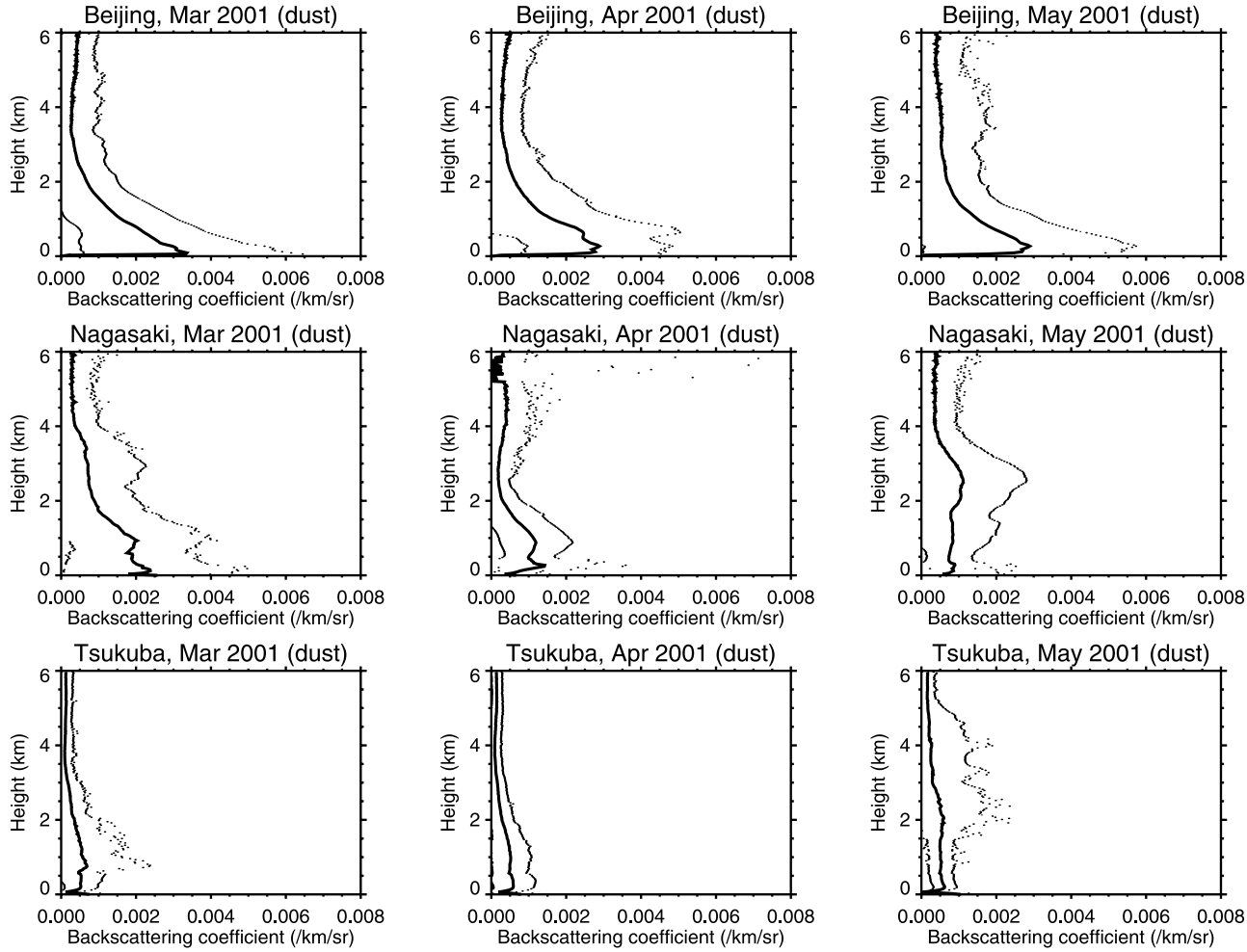

Figure 9. Vertical profiles of averaged backscattering coefficients for dust particles (solid lines) plus or minus standard deviations (dotted lines).

δ_2, the contribution of dust to the total backscattering coefficient is [*Chen et al.*, 2001]

$$R = \frac{(\delta_a - \delta_2)(1 + \delta_1)}{(1 + \delta_a)(\delta_1 - \delta_2)}. \quad (2)$$

This value is sensitive to the selection of δ_1 and δ_2 values, which cannot be determined from Mie-scattering theory. We determined them empirically from Figure 8: 0.35 for δ_1 and 0.02 for δ_2. When δ_a was higher than δ_1 or lower than δ_2, R is set to 1 or 0, respectively. R is depending almost linearly on the inverse of δ_1, and δ_1 will vary in a month and at same place. If δ_1 is determined by other measurement, more appropriate results can be expected. However, the purpose of this analysis is not pursuing optical properties of a particle. At least in a typical aerosol events R represents the mixing conditions using general δ_1 introduced here. From equation (2), the backscattering coefficient by dust particles ($R \times \beta_a$) and by spherical particles ($(1 - R) \times \beta_a$) are calculated for each independent profile. The backscattering coefficients for each aerosols are averaged at each height over a month. The vertical profiles of the averaged backscattering coefficients with $\pm 1\sigma$ for March to May are displayed in Figure 9 for dust and Figure 10 for spherical aerosols.

[25] The averaged profiles of dust backscattering in Beijing show that the air there contained most dust at the lowest altitudes (Figure 9). The backscattering decreased from 0.003/km/sr at the surface to 0.0002–0.0004/km/sr around 3–4 km, and the standard deviations near the surface were small compared with those at the other observatories. These characteristics reveal that the surface air of Beijing was consistently affected by dust during the study period. Nagasaki and Tsukuba showed no common characteristics. The variation in height and density of the dust caused these scattering results.

[26] The spherical aerosol were always concentrated near the surface, and the backscattering by spherical aerosols was nearly zero above 3 km at all observatories (Figure 10). The spherical aerosol layer was particularly thin in Beijing. Sometimes the aerosol layer showed a vertical structure, such as a well-mixed boundary layer, in Japan (e.g., March in Tsukuba: April and May in Nagasaki).

4. Comparison With a Numerical Model

[27] The Chemical Weather Forecasting System (CFORS) is a regional transport model with various tracers and aerosols, including SO_2/sulfate, sea salt, volcanic tracers,

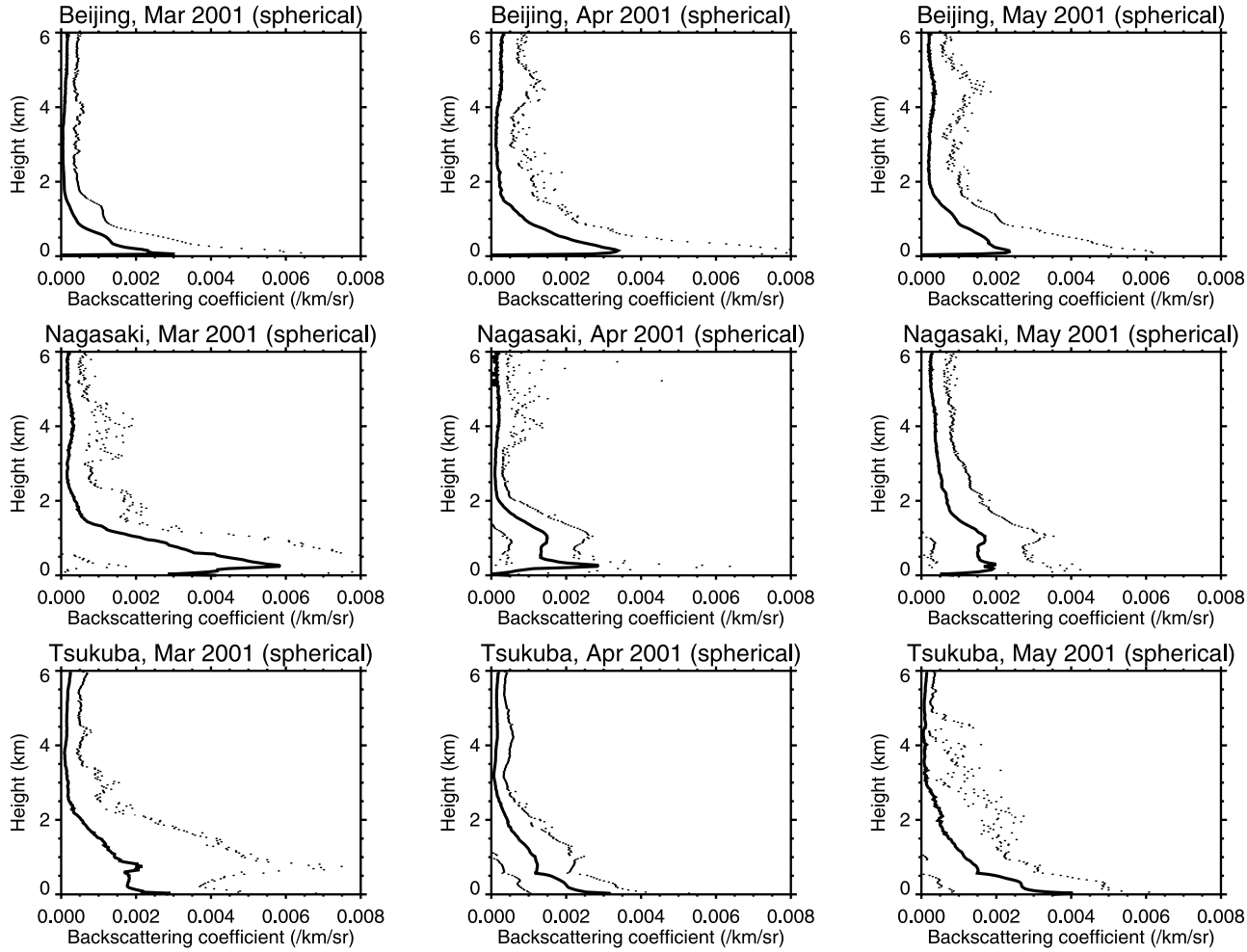

Figure 10. Same as Figure 9 but for spherical aerosols.

CO, black and organic carbon, and mineral dust (12 size bins). It was developed at the Research Institute for Applied Mechanics, Kyushu University [*Uno et al.*, 2003]. CFORS is an online coupled model, incorporating the Regional Atmospheric Modeling System (RAMS) and a chemical transport driver. It is used for real-time forecasting of the three-dimensional distribution of atmospheric components and aerosols to help in the design of measurements at various observation sites. It can also be used to post analysis of the distributions using reanalysis data for atmospheric dynamics. The domain of the calculation is eastern Asia, and the horizontal grid resolution is about 80 km. The vertical resolution varies from about 200 m at the surface to about 2 km at the top of troposphere, and the time step of the output is 3 hours. Source regions of dust emission are identified by land cover data set by U.S. Geological survey, with monthly snow cover data. As a result Gobi and Takla Makan Deserts are indexed as important source region. The anthropogenic emission inventory was based on the data set for ACE-Asia experiment.

4.1. Time Series of Two Kinds of Aerosols in China and Japan

[28] We compared the total dust mass concentration calculated by CFORS with the measured backscattering coefficient due to dust particles. We should mention that the mass concentration does not directly correspond with optical indices such as backscattering coefficient because the optical properties depends on the size distribution of the particles. However, as we separated backscatter into two types of aerosols, this comparison is the first step to infer the conversion factor between mass concentration and optical quantities for dust and spherical aerosols, respectively. Of course, we can utilize some aerosol optical models (e.g., OPAC [*Hess et al.*, 1998]) to calculate mass concentration/backscattering coefficient conversion factor. However, Mie-scattering calculation is applicable for spherical particles only, and size distribution and refractive indices introduced in optical models are compiled from literatures. A direct measurement of aerosol mass near the surface compared with lidar results near the surface with good correction of overlapping factor, are desirable to understand the relationship between model values and remote-sensing results, and to derive the factor. The time-height indications of both in Beijing in April 2001 are shown in Figure 11. In these panels the time-height resolution of lidar results is reduced to that of CFORS. Generally, the tall dust events were well reproduced by CFORS, whereas shallow events, for example that on 1 April, were not. Signals near the surface indicate that the dust event

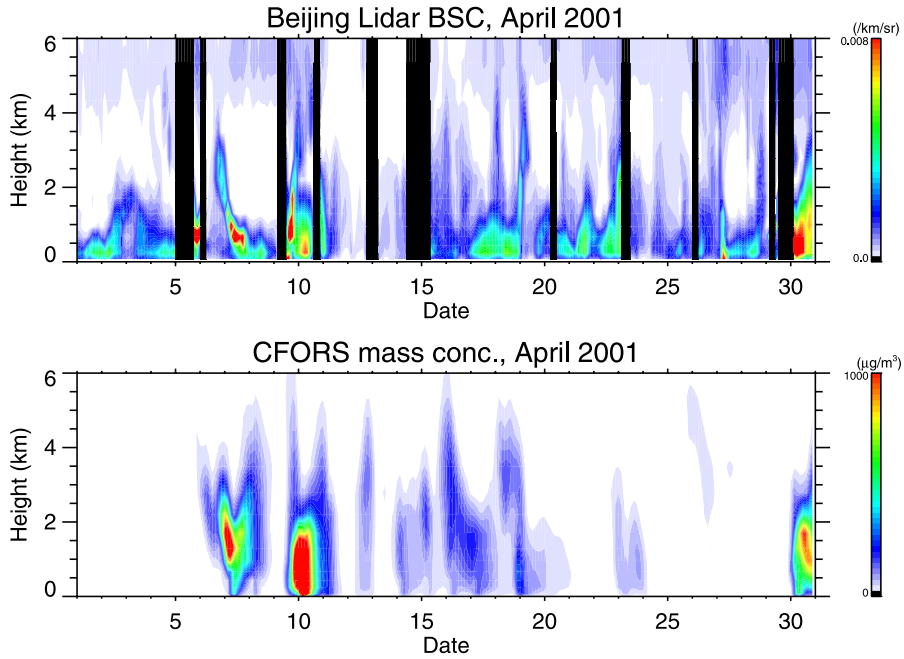

Figure 11. Time-height sections of (top) backscattering coefficient of dust and (bottom) CFORS dust mass concentration in Beijing in April 2001. The black stripes in the top panel show times when the backscattering coefficient was not calculated owing to missed observations or the presence of low cloud.

occurred close to Beijing [*Chen et al.*, 2001]. The tall signals corresponded to transported dust from Gobi and/or Takla Makan Deserts detected after passage of cold trough. This result suggests that CFORS is good at predicting at the transport of dust from the center of the continent to Beijing, but not so good at predicting local events. Figures 12 and 13 show the results for Nagasaki and Tsukuba. Some of transported dust in the free troposphere seen in the lidar results (e.g., on 23 April in Nagasaki and on 1 April in Tsukuba) did not appear in the model results. As all of the dust detected over Japan is considered to be transported, the long distance between the source and Japan caused the discrepancy between model and observations. The differences between model and lidar results both near the source (Beijing) and far away (Nagasaki and Tsukuba) indicate characteristics of the model calculation, and may contribute the further tuning of the model. CFORS correctly predicted dust near the surface in Nagasaki and Tsukuba on 12 and 13 April. Similar

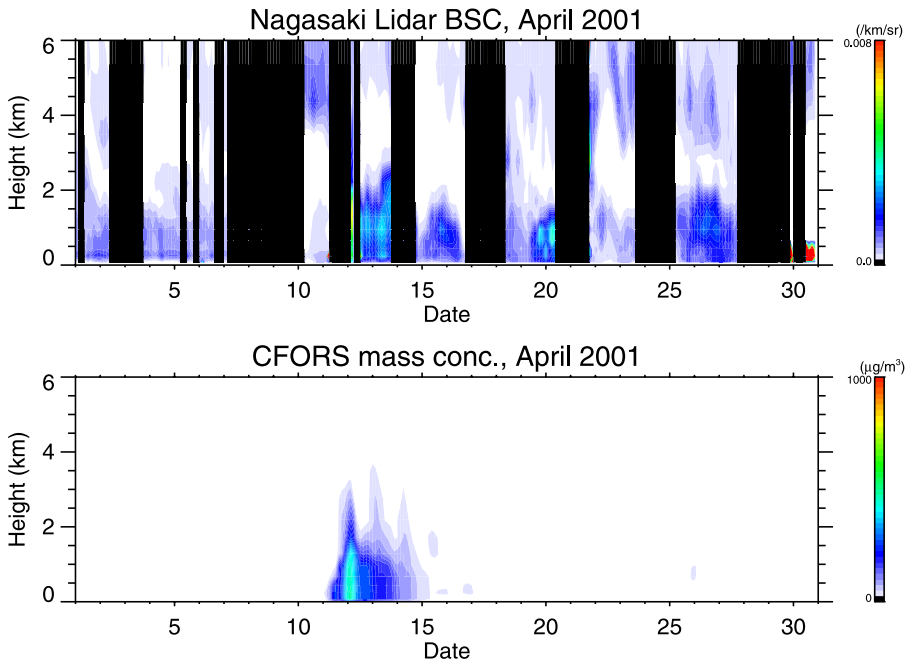

Figure 12. Same as Figure 11, but for Nagasaki.

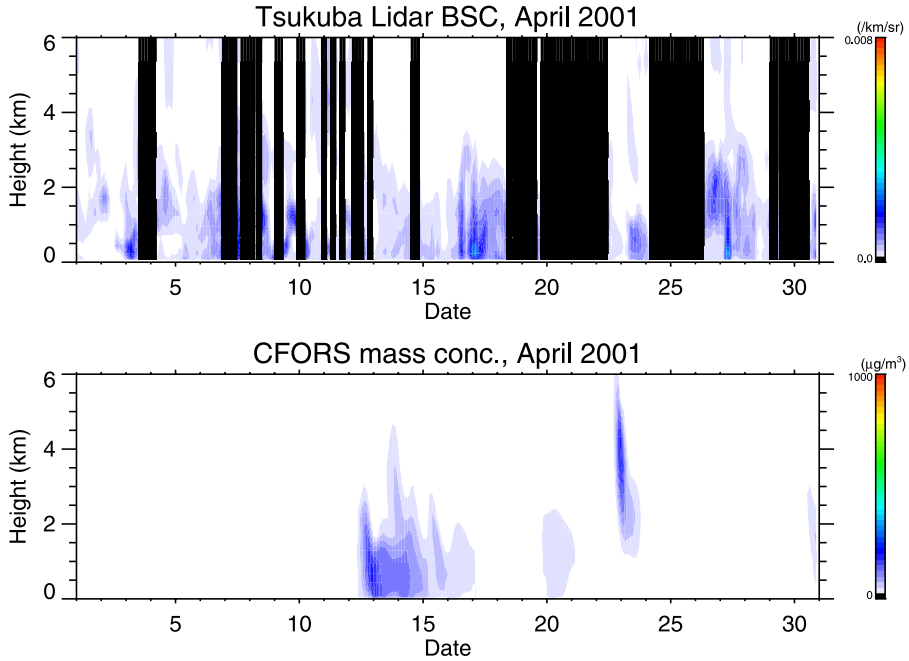

Figure 13. Same as Figure 11, but for Tsukuba.

structure was confirmed in the lidar results. Generally, dust events triggered by the passage of a depression near the Gobi Desert coincided well between the model and lidar results.

[29] Sulfate is one of major constituents of fine particles in the troposphere [*Heintzenberg*, 1989], existing as spherical, water-soluble droplets. We compared the observed backscattering coefficient due to spherical aerosols with the mass concentration of sulfate calculated by CFORS. Figure 14 shows that results for Beijing agreed well, although CFORS predicted a thicker dense layer. The results for Nagasaki and Tsukuba (Figures 15 and 16) showed a good match. The spherical aerosols and sulfate occurred continuously below 1.5–2.0 km, sometimes higher.

4.2. Horizontal Fine Structure of a Specific Dust Event in Japan

[30] The above lidar observations were made at only three sites, and horizontal resolution of CFORS is 80 km. In estimating the effect of the difference in spatial (horizontal) representativity of lidar and CFORS, investigation of the

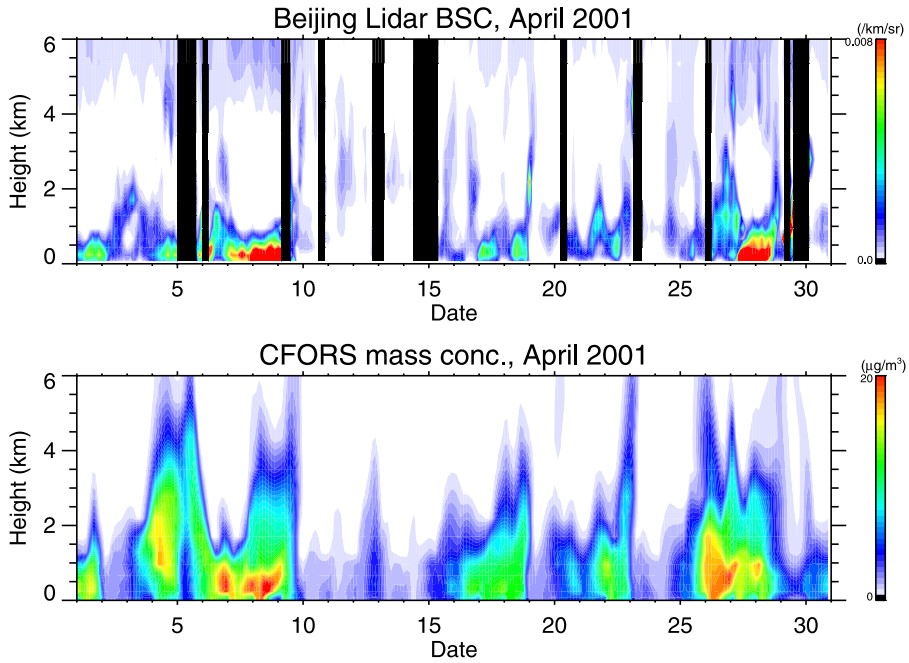

Figure 14. Time-height sections of (top) backscattering coefficient of spherical aerosols and (bottom) CFORS sulfate mass concentration in Beijing in April 2001.

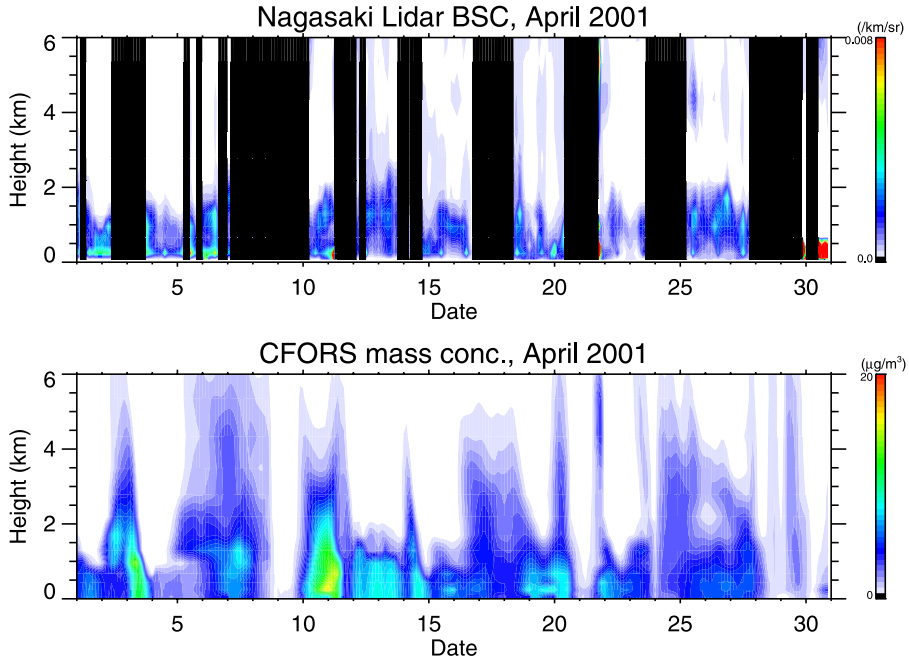

Figure 15. Same as Figure 14, but for Nagasaki.

fine structure of an aerosol plume is important. A dust plume arrived in Nagasaki on 16 May 2001 and in Tsukuba 1 day later. On these days, we used five lidars in central and western Japan to carry out a fine assessment. Four of them were almost equally separated. The lidar in Tokyo is useful for estimating local influence because the distance to Tsukuba is only about 60 km.

[31] Time-height sections of the dust backscattering coefficient in Figure 17 show the fine structure of this dust plume. The backscattering in western Japan (Nagasaki and Fukuyama) was greater than that in central Japan (Shigaraki, Tokyo, and Tsukuba). The dust layer was little thicker in the west, and a floating thin layer was found above the main layer in Tokyo and Tsukuba. Because of the short distance between Tokyo and Tsukuba, their results were similar. Comparison between the lidar observations and CFORS prediction (Figure 18) indicates the reproducibility of the fine structure by the model. In this period, two depressions passed at the north and south of Japan, and the dust region between them was strongly stretched and deformed. The depth of the dust layer is well reproduced in the model at all points, but the timing of maximum

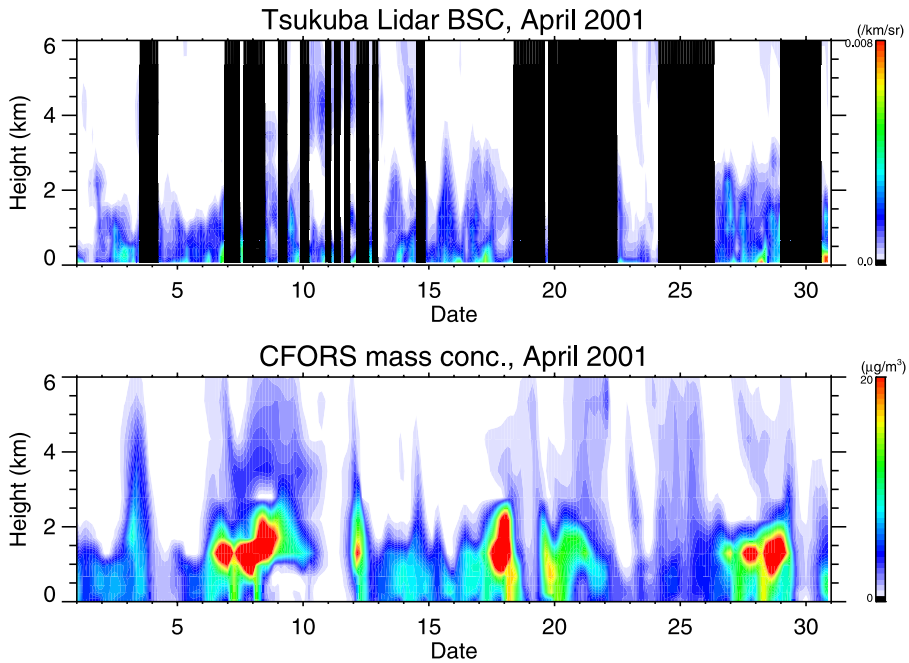

Figure 16. Same as Figure 14, but for Tsukuba.

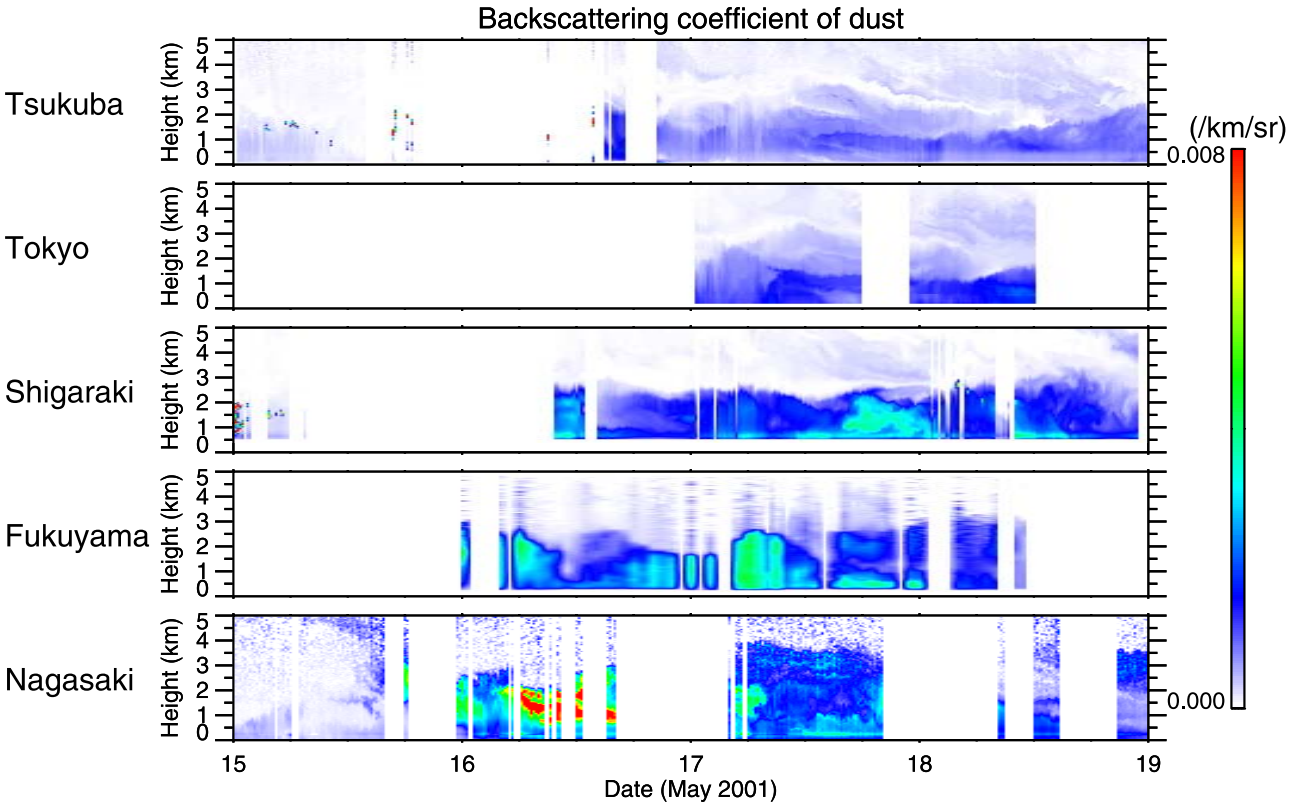

Figure 17. Time-height sections of backscattering coefficient of dust during severe dust event during 16–19 May 2001 in Tsukuba, Tokyo, Shigaraki, Fukuyama, and Nagasaki.

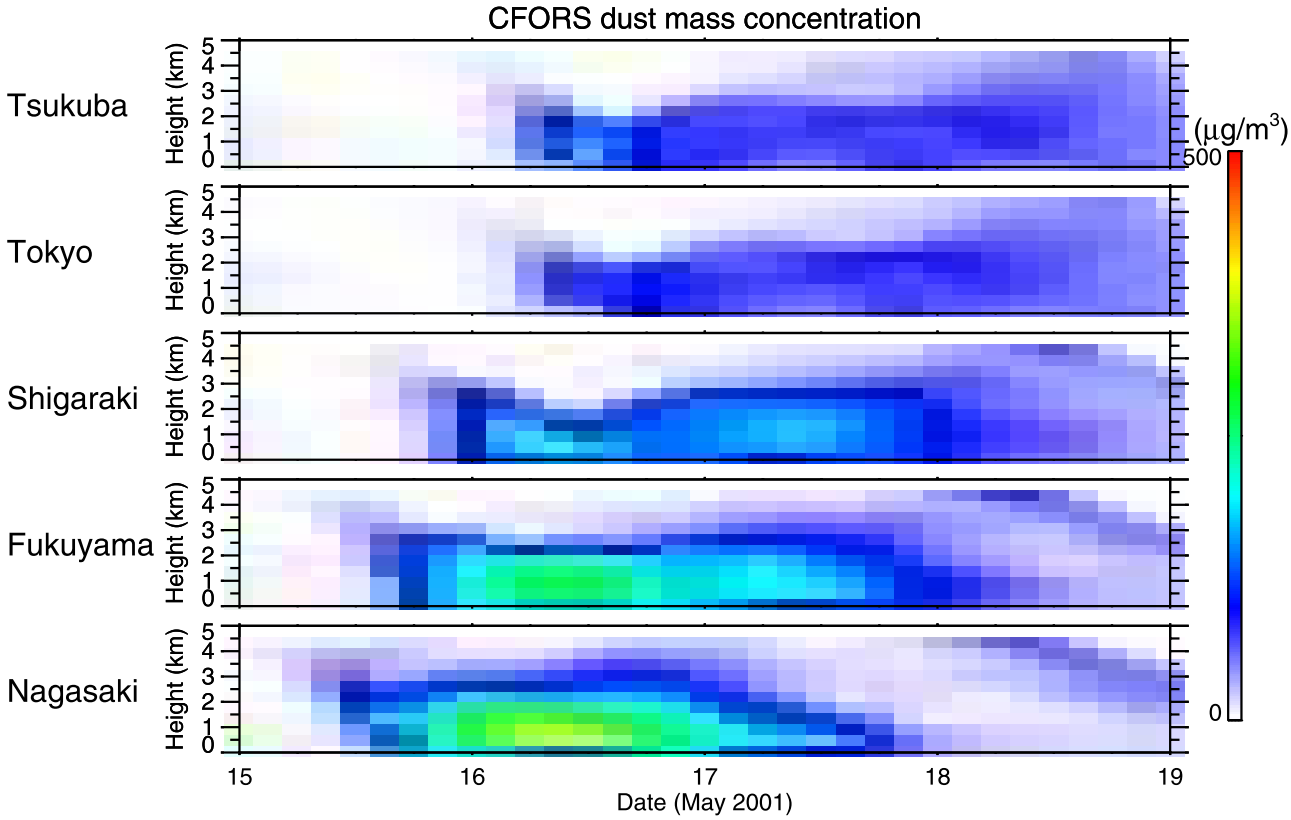

Figure 18. Time-height sections of total dust mass concentration during severe dust event during 16–19 May 2001 at Tsukuba, Tokyo, Shigaraki, Fukuyama, and Nagasaki.

backscattering and maximum mass concentration differs. For example, in Fukuyama and Shigaraki the maximum comes earlier in the model. The inner structure of a dust plume, and the lidar observation at a certain point, may be influenced not only by the large structure of the atmosphere but also by mesoscale phenomena. When we compare the aerosols near the surface predicted by the model and observed by lidar, the difference in spatial representativity must be noted.

5. Concluding Remarks

[32] Continuous polarization lidars were operated in Beijing, Nagasaki, and Tsukuba during the ACE-Asia IOP. The automated lidars obtained vertical profiles during more than 90% of the observation period. Both categorization and quantitative analyses were used to explain the behavior of aerosols and clouds in east Asia. In Beijing, frequent surface dust events reaching up to 4 km occurred, and some of them were transported to the surface in Nagasaki. In Tsukuba, a floating dust layer was observed several times. Qualitative analysis depicted the average structure of optical characteristics of the atmosphere. Backscattering coefficients and δ_a were coupled to estimate the contribution of dust to the total backscattering. Results could be compared with the dust density calculated by a numerical model, CFORS. Comparison showed good agreement for tall dust events in Beijing. CFORS correctly reproduced some surface dust events in Japan and also well reproduced the distribution of spherical aerosols. Finer time-height sections of a specific dust event in May observed by five lidars were analyzed and compared with CFORS predictions.

[33] **Acknowledgments.** All lidar data in Beijing were collected in collaboration with the Sino-Japan Friendship Center for Environmental Protection. Lidar observation at Shigaraki was conducted by courtesy of Takuji Nakamura of the Radio Science Center for Space and Atmosphere, Kyoto University. Authors acknowledge very important and useful comments by the anonymous referees.

References

Browell, E. V., C. F. Butler, S. Ismail, P. A. Robinette, A. F. Carter, N. S. Higdon, O. B. Toon, M. R. Schoeberl, and A. F. Tuck (1990), Airborne lidar observation in the wintertime arctic stratosphere: Polar stratospheric clouds, *Geophys. Res. Lett.*, *17*, 385–388.

Chen, Y., H. Quan, X. Dong, N. Sugimoto, I. Matsui, and A. Shimizu (2001), Continuous measurement of dust aerosols with a dual-polarization lidar in Beijing, in *Proceedings of Nagasaki Workshop on Aerosol-Cloud Radiation Interaction and Asian Lidar Network*, pp. 28–31, Cent. for Environ. Remote Sens., Chiba Univ., Chiba, Japan.

Fernald, F. G. (1984), Analysis of atmospheric lidar observations: Some comments, *Appl. Opt.*, *23*, 652–653.

Heintzenberg, J. (1989), Fine particles in the global troposphere: A review, *Tellus, Ser. B*, *41*, 149–160.

Hess, M., P. Koepke, and I. Schult (1998), Optical properties of aerosols and clouds: The software package OPAC, *Bull. Am. Meteorol. Soc.*, *79*, 831–844.

Husar, R. B., et al. (2001), Asian dust events of April 1998, *J. Geophys. Res.*, *106*, 18,317–18,330.

Iwasaka, Y., H. Minoura, and K. Nagaya (1983), The transport and spatial scale of Asian dust-storm clouds: A case study of the dust-storm event of April 1979, *Tellus, Ser. B*, *35*, 189–196.

Iwasaka, Y., M. Yamato, R. Imasu, and A. Ono (1988), Transport of Asian dust (kosa) particles: Importance of weak kosa events on the geochemical cycle of soil particles, *Tellus, Ser. B*, *40*, 494–503.

Liu, Z., N. Sugimoto, and T. Murayama (2002), Extinction-to-backscatter ratio of Asian dust observed with high-spectral-resolution lidar and Raman lidar, *Appl. Opt.*, *41*, 2760–2767.

Mattis, I., A. Ansmann, D. Müller, U. Wandinger, and D. Althausen (2002), Dual-wavelength Raman lidar observations of the extinction-to-backscatter ratio of Saharan dust, *Geophys. Res. Lett.*, *29*(9), 1306, doi:10.1029/2002GL014721.

Müller, D., K. Franke, F. Wagner, D. Althausen, A. Ansmann, and J. Heintzenberg (2001), Vertical profiling of optical and physical particle properties over the tropical Indian Ocean with six-wavelength lidar: 1. Seasonal cycle, *J. Geophys. Res.*, *106*, 28,567–28,575.

Murayama, T., H. Okamoto, N. Kaneyasu, H. Kamataki, and K. Miura (1999), Application of lidar depolarization measurement in the atmospheric boundary layer: Effects of dust and sea-salt particles, *J. Geophys. Res.*, *104*, 31,781–31,792.

Murayama, T., et al. (2001), Ground-based network observation of Asian dust events of April 1998 in east Asia, *J. Geophys. Res.*, *106*, 18,345–18,359.

Murayama, T., et al. (2002), Lidar network observation of Asian dust events during ACE-ASIA intensive observation period, in *Proceedings of Sixth International Aerosol Conference, September 8–13, 2002, Taipei, Taiwan*, pp. 1215–1216, Chin. Assoc. for Aerosol Res. in Taiwan, Dep. of Chem. Eng., Yuan Ze Univ., Chung-Li, Taiwan.

Myhre, G., and F. Stordal (2001), Global sensitivity of experiments of the radiative forcing due to mineral dust, *J. Geophys. Res.*, *106*, 18,193–18,204.

Pelon, J., C. Flamant, P. Chazette, J.-F. Leon, D. Tanre, M. Sicard, and S. K. Satheesh (2002), Characterization of aerosol spatial distribution and optical properties over the Indian Ocean from airborne lidar and radiometry during INDOEX'99, *J. Geophys. Res.*, *107*(D19), 8029, doi:10.1029/2001JD000402.

Ramanathan, V., et al. (2001), Indian Ocean Experiment: An integrated analysis of the climate forcing and effects of the great Indo-Asian haze, *J. Geophys. Res.*, *106*, 28,371–28,398.

Russell, P. B., P. V. Hobbs, and L. L. Stowe (1999), Aerosol properties and radiative effects in the United States east coast haze plume: An overview of the Tropospheric Aerosol Radiative Forcing Observational Experiment (TARFOX), *J. Geophys. Res.*, *104*, 2213–2222.

Sakai, T., T. Shibata, S.-A. Kwon, Y.-S. Kim, K. Tamura, and Y. Iwasaka (2000), Free tropospheric aerosol backscatter, depolarization ratio and relative humidity measured with the Raman lidar at Nagoya in 1994–1997: Contributions of aerosols from the Asian continent and Pacific Ocean, *Atmos. Environ.*, *34*, 431–442.

Shimizu, H., Y. Iikura, Y. Sasano, and N. Takeuchi (1981), Resolution improvement in an analog-to-digital converter by the superposed dither signal, *Trans. Inst. Electron. Commun. Eng., Sect. E*, *J64-A*, 963–969.

Sugimoto, N., I. Matsui, A. Shimizu, I. Uno, K. Asai, T. Endoh, and T. Nakajima (2002), Observation of dust and anthropogenic aerosol plumes in the Northwest Pacific with a two-wavelength polarization lidar on board the research vessel *Mirai*, *Geophys. Res. Lett.*, *29*(19), 1901, doi:10.1029/2002GL015112.

Uno, I., H. Amano, S. Emori, K. Kinoshita, I. Matsui, and N. Sugimoto (2001), Trans-Pacific yellow sand transport observed in April 1998: A numerical simulation, *J. Geophys. Res.*, *106*, 18,331–18,344.

Uno, I., et al. (2003), Regional chemical weather forecasting system CFORS: Model descriptions and analysis of surface observations at Japanese island stations during the ACE-Asia experiment, *J. Geophys. Res.*, *108*(D23), 8668, doi:10.1029/2002JD002845.

K. Aoki, Faculty of Education, Toyama University, 3190 Gofuku, Toyama, 930-8555 Japan. (kazuma@edu.toyama-u.ac.jp)

K. Arao, Faculty of Environmental Studies, Nagasaki University, 1-14 Bunkyo-machi, Nagasaki, 852-8521 Japan. (araok@net.nagasaki-u.ac.jp)

N. Kagawa, Faculty of Engineering, Fukuyama University, 1 Gakuen-Cho, Fukuyama, Hiroshima, 729-0292 Japan. (kagawa@psws.fuee.fukuyama-u.ac.jp)

I. Matsui, A. Shimizu, and N. Sugimoto, National Institute for Environmental Studies, 16-2 Onogawa, Tsukuba, Ibaraki, 305-8506 Japan. (i-matsui@nies.go.jp; shimizua@nies.go.jp; nsugimot@nies.go.jp)

T. Murayama, Department of Physics, Tokyo University of Mercantile Marine, 2-1-6 Etchu-jima, Koto, Tokyo, 135-8533 Japan. (murayama@ipc.tosho-u.ac.jp)

A. Uchiyama and A. Yamazaki, Meteorological Research Institute, 1-1 Nagamine, Tsukuba, Ibaraki, 305-0052 Japan. (uchiyama@mri-jma.go.jp; akyamaza@mri-jma.go.jp)

I. Uno, Research Institute for Applied Mechanics, Kyushu University, 6-1 Kasuga-kouen, Kasuga, Fukuoka, 816-8580 Japan. (iuno@riam.kyushu-u.ac.jp)